Seal failure and fluid flow in salt-bearing sedimentary basins: A critical example from the Espírito Santo Basin, SE Brazil

Tao Ze[1,2*], Tiago M. Alves[2]

[1] Key Laboratory of Exploration Technologies for Oil and Gas Resources, Ministry of Education, Yangtze University, Wuhan Hubei 430100, China

[2] 3D Seismic Lab, School of Earth and Ocean Sciences, Cardiff University, Main Building, Park Place, Cardiff, CF10 3AT, United Kingdom

Corresponding author: Tel: (+86)13554268778; E-mail: taoze@cug.edu.cn

Abstract

Salt giants are viewed as competent seals for sub-salt fluids. Yet, salt can reveal large inter-crystalline and polyhedral permeability when deeply buried and a certain fluid pressure threshold is reached. This work uses high-resolution three-dimensional (3D) seismic data to explain the processes favouring fluid flow in areas affected by salt tectonics, with emphasis on deformed salt structures offshore Espírito Santo (SE Brazil). Documented fluid flow features include pockmarks, dissolution related pockmarks on the crest of salt structures, gas chimneys, bright spots, polygonal fault systems, and pushed-down reflections within salt structures. Offshore Espírito Santo, fluid was sourced: a) from sub-salt compartments, b) through hydrite dewatering processes, c) through slabs in salt-withdraw basins, d) from deformed strata within salt structures, and e) from supra-salt fluids that migrated through the flanks of salt structures. Focused fluid flow on the crests of salt giants may evolve to active salt intrusion when overburden rocks are < 1200 m thick, depending on the intensity of regional halokinesis. The crests of salt structures are also important fluid flow paths, particularly when developing closely-spaced fault families. As a corollary, the interpreted data show that salt dissolution and intra-salt deformation are important processes accompanying the migration of fluid into faulted supra-salt strata or evolving into active diapirism. Our study has important implications to understand salt seal breaching mechanisms around the globe.

Keywords: SE Brazil; Salt giants; Fluid flow; Deformed salt; Dissolution; Hydrocarbon migration.

Introduction

Salt giants, comprising thick and vast volumes of evaporites (Hübscher et al., 2007), often show acoustically transparent internal reflections in seismic data and, as a result, have been previously regarded as lithological homogeneous (Schoenherr et al., 2007). With new, state-of-the-art seismic data acquisition and processing, the internal character of salt giants has been addressed in more detail for the past few years (Van Gent et al., 2011, Fiduk and Rowan, 2012, Bertoni and Cartwright, 2007, Jackson et al., 2014, Kirkham et al., 2022). Recent studies on salt tectonics indicate that salt rock is impure (Schoenherr et al., 2007, Davison, 2009, Warren and Keith, 2016, Szatmari et al., 2021), and hydrocarbon residuals occur in fractures offsetting these ‘impure’ evaporite intervals (Van Gent et al., 2011, Grishina et al., 1998, Schoenherr et al., 2007). New seismic data have also revealed seismically resolved strata and internal deformation within salt giants (Rowan et al., 2019, Alves et al., 2017; Feng et al., 2017, Alsop et al., 2015; Jackson et al., 2014, Strozyk et al., 2012). As proposed by Rowan et al. (2019), layered evaporite sequences (LESs), rather than pure evaporites, better define salt-rich intervals, as proven by many a borehole drilled in salt-bearing sedimentary basins (Feng et al., 2016, Teixeira et al., 2020). High-amplitude intra-salt reflections are thus thought to comprise evaporites with distinct mineralogical compositions (Jackson et al., 2014, Koyi, 2001), or, instead, clastic or carbonate intervals (Rowan et al., 2019).

The clearer imaging of salt structures in new, state-of-the-art 3D seismic data has also revealed their complex internal deformation (Pontes et al., 2022), at the same time stressing that laboratorial experiments using homogeneous materials do not fully represent the lithological and rheological variability of salt giants. Laboratory experiments indicate that the permeability of salt rock reaches values of nanodarcy (nD) or less (Popp et al., 2001, Kern, 2001). However, with increasing burial depths and elevated temperatures, intercrystalline or polyhedral permeability in rock salt is able to reach that of sandstone at lithostatic fluid pressures (Lewis and Holness, 1996, Hovland et al., 2006, Ghanbarzadeh et al., 2015). Furthermore, dilatancy is promoted in salt intervals that record increasing pore pressures and decreasing effective stress (Davison, 2009). Confirming the results in Borchert and Muir (1964), recent data suggest that leaky salt units may actually prevail in some regions experiencing significant salt tectonics under specific geological conditions. This is the case of regions with important hydrothermal processes (Oppo et al., 2020, Hovland et al., 2006, Hovland et al., 2015, Hovland et al., 2019, Kirkham et al., 2020, Bertoni et al., 2017, Warren and Keith, 2016, Bertoni and Cartwright, 2015) or magma-salt interactions (Magee et al., 2021). Hence, published seismic examples provide evidence for cross-salt fluid leakage in seismic data such as mud volcanos piercing though salt structures, linear fluid chimneys, intra-salt pipe trails, pockmarks at both the base and top of salt structures, and stacked pockmarks (Kirkham et al., 2017, Oppo et al., 2020, Kirkham et al., 2020, Ho et al., 2018, Bertoni et al., 2017, Bertoni and Cartwright, 2015, Davison, 2009, Cartwright et al., 2018, Cartwright et al., 2021). Salt mines have also documented bitumen residuals and hydrocarbon fluid inclusions, indicating that significant fluid migration can occur within salt structures after being sourced from sub-salt intervals (Grishina et al., 1998, Schoenherr et al., 2007),

Fluid flow in sedimentary basins attracts a wide research interest due to its close association with groundwater flow systems, petroleum migration, geothermal reservoirs, ore-forming processes and seabed ecosystems (Dando et al., 1991, Hovland et al., 2010, Hovland and Judd, 1988). The processes behind the release of fluid in sedimentary basins can be instantaneous and catastrophic, or last millions of years to encompass multiple geological processes, including those associated with sediment mobilization, which may last millions of years (Huuse et al., 2010, Andresen, 2012). Fluid flow features are typically identified in seismic data as amplitude anomalies that occur together with a wide range of structures such as pockmarks, mud volcanoes, gas hydrates, chimneys, pipes, sediment injection, carbonate mounds, seeps and related diagenetic phenomena (Cartwright et al., 2007, Løseth et al., 2009, Huuse et al., 2010, Andresen, 2012). Hence, fluid flow features can be classified according to their geometry, lithology, the type of impact on the hosting sediment, as well as after taking into account the mechanisms responsible for their formation (e.g. Andresen, 2012, Huuse et al., 2010, Løseth et al., 2009, Cartwright et al., 2007). Three main groups of seismic scale fluid-flow features, divided according to their formation mechanisms, were summarised by Andresen (2012) as: a) subsurface sediment remobilization, b) vertically focused fluid flow, and c) laterally extensive fluid flow.

The aim of this study is to document intra- and supra-salt fluid flow features in SE Brazil to understand the mechanisms promoting fluid flow in salt-bearing sedimentary basins. We show robust evidence for fluid flow both within deformed salt structures and in supra-salt sediments offshore the Espírito Santo Basin (Fig. 1). Comprehensive models of fluid flow in salt-bearing sedimentary basins are suggested and shown to be potentially applicable to other regions in the world affected by salt tectonics.

Data and methods

The interpreted seismic volume has a high resolution, covering an area of ~ 1890 km^2 in SE Brazil (Fig. 1). Seismic data processing included resampling, spherical divergence corrections and zero-phase conversions, which were undertaken prior to stacking, 3D pre-stack time migration using the Stolt algorithm (Stolt and Benson, 1986) and one-pass 3D migration. The vertical sampling rate for the interpreted seismic volume is 2 ms, for a bin spacing of 12.5 m. With a dominant frequency < 40 Hz, the vertical resolution is estimated to be between 5 and 8 m near the seafloor, and 20 m at the maximum depth of strata investigated in this work (Fig. 2). Constraints on the age of the interpreted horizons are based on the published literature (Fiduk et al., 2004, França et al., 2007, Alves et al., 2009). Key supra-salt stratigraphic markers include: a) an interval of continuous high-amplitude seismic reflections comprising volcaniclastic strata deposited from Eocene to the Late Oligocene (Unit 3), b) a regional Eocene unconformity present throughout the study area (horizon H3), and c) a late Oligocene unconformity of regional expression (horizon H4) (Ze and Alves, 2016, Fiduk et al., 2004) (Fig. 2).

Primary-wave velocity data (Vp) from the Deep-Sea Drilling Program (DSDP) Site 516 are used in this work to calculate the minimum thickness of supra-salt overburden units (Barker, 1983, Alves et al., 2009) (Figs. 1, 3, and 4; Table 1). Overburden strata comprise four units, with the uppermost one showing thick mass-transport deposits (MTDs) (Figs. 3 and 4). An average velocity of 2.5 km/s is used to calculate the thickness of Units 1 and 2 (Fig. 2), which represents strata spanning from the crests of salt structures to the base of the volcaniclastic deposits (Fig. 2). An average Vp velocity of 3.0 km/s is assumed for the volcaniclastic deposits in the study area (Unit 3, Fig. 2). A Vp velocity of 1.6 km/s is assumed for the MTDs, and 2.1 km/s is used for the rest of Unit 4 (Fig. 2).

Regional geological background

The Espírito Santo Basin (ESB) is located on the SE Brazilian continental margin, which was formed in association with Late Jurassic-Early Cretaceous rifting and break-up of the Gondwana supercontinent (Fig. 1). The syn-rift succession in the ESB comprises fluvial-lacustrine strata, including main source rocks in the study area (Fiduk et al., 2004) (Fig. 2). Above this succession, more than 2000 m of Aptian salt were deposited and overlain by Albian carbonates and open marine strata comprising shales, turbidites and MTDs (Chang et al., 1992, Tedeschi et al., 2017, França et al., 2007) (Fig.2).

The supra-salt structure of the ESB was largely influenced by halokinesis, and three domains of extension, diapirism and compression are identified on regional seismic profiles (Fiduk et al., 2004). Halokinesis peaked during the late Cenozoic in most of the Espírito Santo Basin, particularly in its intermediate and distal continental slope where salt diapirs, allochthonous salt canopies, and fairways occur and deform the seafloor (Fiduk et al., 2004) (Fig. 2).

The study area is located in the compressional domain, with salt diapirs, ridges and walls and overhangs comprising primary structures (Fig. 1). The height of interpreted salt structures can reach over 4000 m, and they are actively growing at present (Ze and Alves, 2016). Salt successions can be divided into various units, or layered evaporite sequences (Rowan et al., 2019). Four units of layered evaporite sequence are usually documented in SE Brazil, revealing variable composition and bulk density in salt (Jackson et al., 2015). Intra-salt deformation in these thick salt successions comprise faults and folds with variable limb angles (Davison, 2009, Jackson et al., 2015; Alves et al., 2017).

Seismic stratigraphy

Strata in the study area are divided into four seismic stratigraphic units, which are bounded by five horizons (H1 to H5) (Fig. 2). Horizon H1 represents the top of the Aptian salt, whereas H5 represents the seafloor, with its strong and continuous reflector (Fig. 2). In addition, seismic horizons H1a and H1b are interpreted in Fig. 3e to represent the basal and top surfaces of a salt overhang interpreted in the study area (Fig. 3e). Seismic stratigraphic interpretations were extended to the adjacent salt withdrawal basin in order to constrain the age of the strata on the crest of the salt ridge.

Unit 1 (Late Cretaceous)

Unit 1 is bounded by Horizon H2 at its top and Horizon H1 at its base. It shows strong to moderate amplitude internal reflections, chaotic in places (Fig. 2). The base of Unit 1 is hardly identified in the adjacent salt-withdrawal basins. Its top (H2) coincides with a regional unconformity of early Paleocene (Fiduk et al., 2004, Gamboa and Alves, 2015).

Unit 2 (Paleocene - Early Eocene)

Unit 2 is bounded by a moderate and continuous seismic reflection at its top (Horizon H3, Fig. 2). Internal reflections vary in their characters over the salt ridge. Unit 2, when compared to the adjacent salt-withdrawal basins (Fig. 3), is characterized by its transparent to low amplitude internal reflections above salt structures, but shows strong reflections in adjacent salt-withdrawal basins (Figs. 2 and 3). Unit 2 is composed of prograding sandstones and shales, which are ubiquitous on the SE Brazilian margin (Fiduk et al., 2004; França et al., 2007).

Unit 3 (Mid-Eocene - Oligocene)

Unit 3 is bounded at its base by a mid-Eocene unconformity (H3) and at its top by Horizon H4 (Fig. 2). Strata within this unit show sub-parallel, high-amplitude internal reflections with good lateral continuity (Fig. 2). High-amplitude reflections in this unit are generated by volcaniclastic sediment sourced from the Abrolhos Bank during the Middle Eocene-Oligocene (Gamboa et al., 2010, Fiduk et al., 2004). Unit 3 is faulted on the crest of the salt ridge (Fig. 2) and thickens sharply into the salt withdrawal basins (Figs. 3 and 4).

Unit 4 (Late Oligocene - present)

Unit 4 shows internal seismic reflections of moderate amplitude and is divided into two sub-units (Fig. 2). The lower Unit 4 is bounded at its base by Horizon H4 (Fig. 2). A large number of crestal faults terminates at the base of the MTDs (Figs. 2 and 3). The upper Unit 4b comprises the thickest MTDs (over 200 ms twt or 160 m considering an average velocity of 1.6 km/s) deposited in the study area (Figs. 2 and 3).

Fluid flow features on the crest of salt structures

Bright spots interpreted in seismic data are often fluid accumulations associated with multiple fluid sources (Ze and Alves, 2021). Dim zones are often interpreted as gas chimneys associated with sub-surface fluid flow (Fiduk et al., 2004). However, due to the existence of bright spots lying on top of acoustic transparent zones, seismic artifacts might occur in some given examples. The examples in this study are interpreted to be gas chimneys due to the fact that the configuration of the interpreted acoustic transparent zones and bright spots vary greatly in the study area (Fig. 3). Moreover, considering the high-resolution of the seismic data, the shallow burial depths of the interpreted features, and that bright spots have too small a scale to generate dim zones, gas chimneys are thus interpreted based on the given seismic examples (Figs. 3 and 4). Agreeing with previous research by Fiduk et al., (2004), bright spots stacking on top of gas chimneys are common fluid flow features in the Espírito Santo Basin (Fiduk et al., 2004) (Figs. DR1 and DR2). Circular sags are interpreted as dissolution pockmarks and present diameters of 700 m and 400 m, respectively (Fig. 3-5 and DR2). Collapsed sediment filled these pockmarks (Fig. 3e), and sediment thickness increases where the pockmarks were developed (Figs. 5b and 5c). The pushed-down reflections in Figs. 2, 3e and 4 are symmetric, and of a smaller scale to the ‘typical’ intra-salt deformation styles of SE Brazil (Figs. 4). The scales of the pushed-down reflections also correlate with the presence of dissolution pockmarks on the crest of the salt diapir, which are herein postulated to be associated with fluid flow (Fig. 4). The pushed-down reflections in the given example also show good correlation with the high-amplitude anomalies at their roots, and are closely associated with deformed strata in the salt structure (Fig. 4).

The detailed analysis of the seismic features reveals that fluid flow features in this study mostly comprise gas chimneys (Figs. 3, 4 and 6), or are, instead, associated with polygonal faults (Figs. 3e and 5a), pockmarks on top of salt structures (Fig. 3e, 3h, 4, 5 and DR2), bright spots (Figs. 3, 4, 6 and 7), and active salt intrusions (Fig. 8). The geometry of supra-salt fluid flow features often reveals pockmarks on the crests of salt diapirs, with gas chimneys and bright spots stacking on their tops (Figs. 3e, 3h, and DR1).

Gas chimneys in the study area show cylindrical shapes, with diameters of c. 551 m, 1406 m, 737 m, and 1077 m respectively (Figs. 3e -3h). In the case of Fig. 3h, the diameter at the base of the gas chimney is larger than in its upper part (Fig. 3h). The thickness and locations of bright spots lying on top of the gas chimneys vary greatly in the study area, with most located directly on top the gas chimneys. In Fig. 3f, bright spots stretch further upward (Fig. 3f). In Fig. 3h, bright spots are observed in both the western side and top of the latter gas chimney (Fig. 3h).

Fig. 4 presents an example of a fluid flow system in which pushed-down reflections are observed within the salt structures (Fig. 4), with two pockmarks lying directly on top of the same salt structure (Figs. 4 and 5), which were filled by collapsed sediment (Fig. 3e). A gas chimney, present on top of the pockmarks on the crest of the salt overhang, stretches through the supra-salt successions, and ends in

Unit 4 (Fig. 4). A crestal fault system is developed in the supra-salt succession, with a polygonal fault system offsetting Units 2 - 3, and terminating in Unit 4 (Figs. 4 and 5a). Isopach maps of Unit 1 and unit 2 show apparent strata thickening on top of the pockmarks (Fig. 5c). The root of the interpreted pushed-down reflections is located on top of high-amplitude anomalies within the salt structures, which are part of the deformed intra-salt structures (Fig. 4)

Apart from the fluid flow system shown in Fig. 4, simpler fluid systems with a gas chimney lying at the structural high on the crest of salt structures, and bright spots lying on top of the gas chimneys are identified throughout the study area (Figs. 3f - 3h).

Active, buried salt intrusions revealing significant fluid flow

Figs. 6 and 7 present unique examples of buried salt intrusions, which have a minor influence on current seafloor morphology (Figs. 6 and 7). Active salt intrusions shaping the modern seafloor are also observed in the study area (Fig. 8). The active salt intrusion pierced through supra-salt successions, forming an anticline at the modern seafloor (Fig. 8). A crestal fault with a maximum throw value over 100 ms twt is interpreted on the north flank of the active salt intrusion (Fig. 8). Internal reflections in the latter correlate with the salt diapir lying below the salt intrusion in Figs. 6 and 7. However, they show partially continuous internal reflections that are parallel to its host supra-salt strata (Figs. 6 and 7). Further north, the salt intrusion in Fig. 7 changes into a gas chimney (Figs. 1 and 3g). A tilted gas chimney located in the salt withdrawal basin is also identified in Fig. 8.

Location of fluid flow features

The study area is located in the compressional zone of the Espírito Santo Basin, which is currently experiencing significant halokinesis (Ze and Alves, 2016). As a result, most supra-salt strata are highly faulted, with salt flowing towards the seafloor (Fig. 8). The observed examples of focused fluid flow are mostly located on top of large salt diapirs (Figs. 1, 3, 4 and 6). An important detail is that where the gas chimneys occur, the thickness of supra-salt units is relatively similar, approaching 1600 m (Fig. 3e), 1450 m (Fig. 3f), 1650 m (Fig. 3g), 1750 m (Fig. 3h) and 1450 m (Fig. 7), after converting two-way time (twt) thickness to true thickness using velocity data from DSDP Site 516 (Barker, 1983) (Table 1).

Horizon 4 is interpreted to be Late Oligocene in age, with continuous, high-amplitude strata below representing volcaniclastic material deposited from the Eocene to Late Oligocene (Ze and Alves, 2016, Fiduk et al., 2004) (Fig. 2). Bright spots in Figures 3e, 3f, 4, 6 and 7 are observed in Unit 4, and the gas chimney pierced through the brittle volcanoclastic unit (Figs. 3e, 3f, 4 and 7, Table 1). In Fig. 3g, bright spots are located within the volcaniclastic Unit 3, a character indicating that the marine mud-rich succession above comprises a seal interval. However, in Fig. 3h bright spots extend from Unit 2 to Unit 4, and show a geometry that is different from other bright spots of the same kind (Fig. 3h).

Deformed intra-salt structures and intra-salt anomalies

Intra-salt seismic anomalies comprise mainly pushed-down reflections (Figs. 3e and 4), deformed strata (Figs. 4 and 6), and relatively continuous high-amplitude reflections in intra-salt strata (Figs. 8 - 10). High-amplitude intra-salt strata are interpreted to be volcanoclastic/clastic deposits (Fiduk et al., 2004), or rafts (Jackson et al., 2014). However, the examples given by Jackson et al. (2015) also indicate that high-amplitude reflections are due to different salt compositions. With the example in Fig. 6, the highly tilted intra-salt reflections are postulated to be reflections by the layered evaporite sequences (Rowan et al., 2019), which are important intra-salt fluid migration pathways (Fig. 6).

Fig. 9 and Fig. 10 present two different types of intra-salt high amplitude anomalies (HAAs). In Figure 9, high-amplitude anomalies are continuous in section view (Figs. 9a and 9b). In map view, HAAs are confined within the salt structures, with their geometries showing strips within the salt structures (Fig. 9c), while in Fig. 10, HAAs are small circular dots in cross-section and map view (Fig. 10). HAAs of these two types are common throughout the Espírito Santo Basin (Fig. 3, 4 and Figs. 6 - 10).

Discussion

The study area records significant halokinesis and comprises sub-salt strata that form the reservoirs with the largest economic importance in SE Brazil (Fiduk et al., 2004). We support the idea that even though salt giants often comprise perfect seals for fluid flow, they can also bear sufficient fluid, and act as direct paths for fluid flow into shallower successions. As indicated by outcrop data (Schleder et al., 2008) and seismic studies (Bertoni and Cartwright, 2015, Davison, 2009, Strozyk et al., 2012), if fluid pressure reaches a critical value or a percolation threshold is reached, pore networks within salt diapirs become connected, enhancing the permeability of salt structures and allowing fluid to be transferred within salt structures (Ghanbarzadeh et al., 2015, Popp et al., 2001, Smodej et al., 2019). Bitumen residuals have been widely documented within salt rock (Flambard et al., 1986, Schoenherr et al., 2007). Furthermore, internal deformation is prevalent and complex within salt structures (Alves et al., 2017, Dooley et al., 2015, Rowan et al., 2019). When deformation of more porous layers in salt successions occurs, creating hydraulic-pressure gradients, fluid flow is more likely to occur within salt giants. Other fluid flow features piercing thick evaporites are also documented in the form of mud volcanoes in the Nile delta, and vents in offshore areas of SE Brazil (Kirkham et al., 2020, Kirkham et al., 2017, Alvarenga et al., 2016).

To better understand fluid flow in salt sedimentary basins, this study interprets abundant and plentiful fluid flow features in the Espírito Santo Basin. New insights on the fluid sources generating these fluid flow features, and the processes and mechanisms for fluid flow in both intra- and supra-salt successions, are key to the further investigation of fluid flow in salt-bearing basins.

Distinct fluid flow mechanisms in salt-bearing basins

The 3D configuration of the pre-salt topography high (Fig. DR1), intra-salt high-amplitude anomalies, deformed intra-salt strata, pushed-down reflections, dissolution pockmarks, polygonal faults and bright spots on top of the gas chimney in this study, agree with the inference that fluids forming these focused fluid-flow events were often originated from multi-fluid sources, both from pre-, within- and supra-salt successions (Fig. 4). With this setting in mind, an interesting and vital question is how multiple fluid sources contribute to fluid flow in salt-bearing sedimentary basins?

Sub-salt strata bear large volumes of fluid in underlying structural traps in the Espírito Santo Basin (Fiduk et al., 2004), a character generating excess pore pressure underneath salt diapirs. As shown in Alves et al., (2017), topography highs often develop at the base of salt structures, favoring the accumulation of fluids underneath thick salt successions (Alves et al., 2017; Fiduk et al., 2004). If the accumulated fluid comprise mainly water, dissolution-related fluid migration can pierce through the salt structures and form pockmarks both at the base and top of salt diapirs (Bertoni and Cartwright, 2015, Kirkham et al., 2017). Mechanisms for such a process are summarized in Kirkham et al. (2017, 2020), which focused on analyzing large mud volcanoes piercing through thick evaporite seal units. Bertoni and Cartwright (2015) also pointed out that dissolution pockmarks might exist at both the base and top of the evaporite succession. This mechanism is partially proved by the presence of pockmarks on the crests of the salt structures in the study area (Figs. 3e and 3h), which direct fed fluid into salt structures and being migrated further upward from pre-salt compartments. This, the deformed pre-salt strata could significantly contribute to fluid flow (Fig. DR1 and 4). Hydrothermal fluid, including hot brines could have also migrated through salt structures in the Espírito Santo Basin (Schoenherr et al., 2007, Hovland et al., 2006, Hovland et al., 2015). Sub-salt successions in the Espírito Santo Basin are known to trap large reserves of oil and gas (Fiduk et al., 2004). If the accumulated fluids comprise mainly oil and gas, a mechanism breaching the pressure threshold of the observed salt units may be crucial, as high-magnitude overpressured oil and gas will lead to increases in the inter-crystalline and polyhedral permeability of salt structures, favoring the transfer of sub-salt fluid into 'impure' and 'deformed' salt (Lewis and Holness, 1996, Ghanbarzadeh et al., 2015). The burial depths of the salt structure in the Espírito Santo Basin can reach over 7000 m (Fig. 4 and DR1), meaning that the base of salt structures record an overburden loading of over 140 MPa, with high temperatures contributing to the breaching of the salt structures. This also means that oil, gas and hot fluids (basinal brines and condensation water) could have flowed into the salt structures (Hovland et al., 2006, Hovland et al., 2018 a, b, Hovland et al., 2019, Ghanbarzadeh et al., 2015, Lewis and Holness, 1996).

A second possible source of fluid in salt structures relates to dehydration processes of gypsum into anhydrite (generating water), and maturation of organic matter in intra-salt sediment packages (generating hydrocarbons). Thin layers of black shales are known to exist in thick evaporite succession in the Espírito Santo Basin, as well as in other basins with significant salt (Fiduk et al., 2004). Rock salt is thermally conductive (Barry et al., 1998), indicating that even if organic matter in adjacent salt-withdraw basins does not reached the maturation window, organic matter in intra-salt strata may be able to generate oil and gas (Fig. 4). Either explanation for the HAAs observed within the salt structures, means that large volumes of fluid, including water and hydrocarbons, may be generated in salt giants as observed in the study area (Figs. 3, 4, 9 and 10).

A third contribution to supra-salt fluid flow relates to fluid generated in supra-salt successions, from polygonally faulted intervals to fluids migrating along salt flanks and along fault systems formed on these same salt flanks. As salt welds are commonly developed in the Espírito Santo Basin, sub-salt fluid might have migrated first into supra-salt strata, contributing later to the formation of fluid flow features on the crest of salt structures (Hudec et. al., 2007).

A comprehensive fluid flow system in salt tectonics

The geometry associated to pushed-down seismic reflections, mega-dissolution pockmarks (with a diameter of ~ 1200 m, Figs. 3a, 4 and 5b), circular areas in the isochron maps of key stratigraphic units on top of the salt structures (Figs. 5c and d), gas chimneys (Fig. 3), polygonal faults (Fig. 5a) and bright spots (Figs. 3, 4, 6 and 7) indicate significant fluid flow and a comprehensive fluid flow system in the study area. Due to the high-velocity of evaporites, and difficulty in imaging internal salt structures, internal salt reflection geometries often return varied interpretations (Rowan et al., 2019, Hovland et al., 2018a, b). Pulled-up seismic reflections, rather than pushed-down due to velocity contrast between salt deposits and their overburden sediments, exist within salt structures (Li and Mitra, 2020). Here, we argue the pushed-down reflections within salt structures, and giant pockmarks on the crests of these latter, agree with data from the Mediterranean Sea (Bertoni and Cartwright, 2015), and relate to the localized (dissolution-related) upward migration of fluids (Hovland et al., 2015, Hovland et al., 2018a, b, Hovland et al., 2019) (Fig. 4). Hydrothermalism, refering to possible contributions of volatiles and metals from underlying magma chambers, has been proposed by various case studies as a source of fluids migrating into salt structures (Schoenherr et al., 2007, Hovland et al., 2006, Hovland et al., 2015, Magee et al., 2021). The Espírito Santo Basin experienced various episodes of volcanism, and salt structures in this basin are often associated with high heat-flow events and volcanic intrusions. In addition, structural highs were often developed beneath salt giants, favoring the focusing of fluid pressure (Fiduk et al., 2004; Alves et al., 2017,) (Fig. DR1). As shown by Fiduk et al. (2004), high overpressure may occur beneath the pre-salt topography-high, where sub-salt fluid migration into the salt structures occurred. Together with deformed intra-salt strata, significant fluid flow may occur, forming the pushed-down reflections observed in this study (Figs. 4 and DR1). Apart from Fig. 3e, Figure 3h presents a mega-pockmark with a diameter over 1000 m on the crest of a salt diapir. Internal salt deformation in Fig. 3h is associated with pushed-down seismic reflections that, similarly to Fig. 3a, suggest fluid flow through salt to be one of the main processes contributing to salt seal failure (Fig. 3h).

Figure 7 presents an example of a salt intrusion with bright spots lying on its top. The salt intrusion, moving further north, changes into a gas chimney at the highest point of the salt structure (Fig. 3g), indicating that. in this case, the intrusion of salt was accompanied by significant fluid flow (Figs. 3g and 7). Pockmarks on the crest of the salt giants (Figs. 3e and 3h), pushed-down reflections in salt giants (Fig. 3e), salt intrusions accompanied by significant volumes of fluid (Figs. 3g and 7), and the known hydrothermal fluid percolating into salt structures (Hovland et al., 2006, Hovland et al., 2015), support the idea that fluid flow through salt might be prevalent in salt-bearing basins under particular conditions.

Although fluid flow through the salt is inferred in the study area, we cannot ignore the contribution of a significant volume of fluids derived from supra-salt strata. Polygonal faults are direct evidence that a significant volume of fluid was expelled from the strata bearing these fault systems (Figs. 3e and 5) (Berndt et al., 2003; Berndt and Gay, 2007). Thinned strata over supra-salt structures suggest important contribution of differential compaction, with polygonal faults contributing to fluid flow (Cartwright, 2011, Cartwright et al., 2003, Cartwright and Lonergan, 1996). Migration of fluids along the flanks of salt structures, and bypass fault systems along salt flanks, are other mechanisms that generating fluid flow features.

Overburden loading as a key control of focused fluid flow in supra-salt strata

Based on the results of this study, we propose conceptual models for fluid accumulation and flow through giant salts based on the interpreted data from SE Brazil (Fig. 11). The first model considers that large volumes of fluid sourced from the sub-salt successions flow into the salt giants, a phenomenon promoted by processes such as hydrothermal-fluid breaching, dissolution-related fluid breaching and pressure-threshold breaching (Figs. 11a and 11b). A second model considers that fluid was sourced from within the salt structures, including fluid from dehydration processes, maturation of organic matters within intra-salt strata, and the migration of fluid from salt-withdrawal basins to porous intervals in the salt structures (Figs. 11c, 11d and DR1). Seismic features marking these processes include deformed intra-salt strata, intra-salt high-amplitude anomalies, pushed-down reflections within the upper part of salt structures, pockmarks on the crest of salt structures, gas chimneys on top of the dissolution pockmarks, and bright spots on top of the gas chimneys (Fig. 11).

As indicated previously, focused fluid-flow events were often originated from multi-fluid sources, both from pre-, within- and supra-salt successions. Our study indicates that fluid flow through salt contributes to the formation of bright spots in supra-salt successions, however, fluid flow forming the gas chimney and bright spots in the study area should also source from supra-salt fluids from the salt withdrawal basins migrating along the salt flanks, or sub-salt fluid migrating through salt welds and along salt flanks (Fig. 11d). For example, the relative absence of dissolution pockmarks on the crest of salt structures indicate that some of the fluids are from supra-salt successions (Figs. 3g and 3h).

Crestal faults are well developed in the study area (Figs. 3 and 4). This type of faults are active conduits for fluid flow. As indicated by Ze and Alves (2016), border faults show the largest throw values within a crestal fault system, and remain active during the propagation of crestal fault system. The active salt intrusion in Fig. 8 presents one of the best published examples of salt using crestal faults on top of the salt to intrude younger strata (Fig. 8). The yellow line in Fig. 8 indicates the relative location of a main crestal fault with a throw value of over 100 ms (twt). This particular crestal fault has an abnormally large throw, a character defining it as a border fault on the crest of the salt diapir. In this case, the active salt intrusion is likely to have used this crestal fault as a weak point for salt to intrude (Fig. 8). However, as indicated in the previous section, salt intrusion is also associated with significant fluid flow.

Regardless of a thermogenic or diagenetic origin for fluid, our seismic interpretation and statistics for supra-salt thicknesses suggest that focused fluid flow will form gas chimneys above salt giants when at least two critical conditions are observed: 1) a minimum thickness of overburden strata occurs on top of the salt structures, 2) large crestal fault systems are developed, namely border faults (Ze and Alves, 2016). Even though the overburden thickness in which fluid chimneys are observed off Espírito Santo reaches values between 1450 m and 1750 m (Table 1), these same values should vary elsewhere in SE Brazil. Where active salt intrusions occur, overburden loading is ~ 1200 m, a value smaller than that of forming gas chimneys (Fig. 8 and Table 1). We therefore postulate that if overburden strata is thinner than a certain value, or pressure imposed by growing salt increases, active salt intrusion, and associated fluid-flow, should predominate through salt giants (Fig. 8).

Conclusions

Our research documents a series of significant fluid-flow features offshore the Espírito Santo Basin. Our understandings of these fluid flow features are closely associated with salt seal failure, and fluid flow through salt. The main results of this paper are summarized as follows:

1) Fluid flow systems chiefly comprise pushed-down seismic reflections in thick salt, dissolution pockmarks on the crest of salt structures, gas chimneys, bright spots, and active salt intrusions that accompany fluid flow. These fluid flow features have 3D geometries that are vertically stacked.
2) The source of fluid within salt giants can be: a) subsalt fluids that breaches into salt structures either by dissolution or by exceeding a certain salt pressure threshold, b) fluids generated by dehydration processes within salt giants, or by maturation of organic matter within clastic sediment packages in salt; c) fluid migrating from salt-withdrawal basins into strata within salt structures.
3) It is not feasible to exclude, in the study area, fluid sourced from salt withdrawal basins, migrating along salt flanks, or from sub-salt strata that migrate through salt welds and along salt flanks into supra-salt successions.
4) Focused fluid flow will form gas chimneys above salt under, at least, two critical conditions: a) a minimum thickness of overburden strata on top of the salt structures, b) the generation of large crestal fault systems. With lower overburden loading, active salt intrusions will replace the formation of gas chimneys.

Our study proposed models that fluid flow can penetrating thick salt structures, however, we also recognized that contributions of supra-salt fluids are significant for fluid flow systems in salt-bearing basins. Indications of fluid flow through salt has very important meanings to reevaluate how geological processes, such as hydrothermal processes and volcanisms contributes to fluid flow systems in salt sedimentary basins. Moreover, salt seal breaching comprises an important risk to petroleum exploration in pre-salt successions, especially in areas with thinner, more deformed salt. Nevertheless, such a setting also offers opportunities for sub-salt oil and gas to accumulate in supra-salt successions via their migration through ‘impure’, deformed evaporites.

Acknowledgements

We thank CGG for the permission to use the seismic data in this paper. Schlumberger (Petrel®) is acknowledged for the provision of using the related software in completing this piece of work. We acknowledge the constructive comments of the editors and reviewers, that greatly improved the quality of the paper. The publication of this work was supported by the China National Natural Science Foundation project No. 41902198 and the China Postdoctoral Science Foundation project No. 2019M662738. The authors thank the colleagues in the 3D Seismic Lab at Cardiff University for the help and tips provided.

References

ALSOP, G. I., WEINBERGER, R., LEVI, T. & MARCO, S. 2015. Deformation within an exposed salt wall: Recumbent folding and extrusion of evaporites in the Dead Sea Basin. *Journal of Structural Geology,* 70**,** 95-118.

ALVARENGA, R. S., IACOPINI, D., KUCHLE, J., SCHERER, C. M. S. & GOLDBERG, K. 2016. Seismic characteristics and distribution of hydrothermal vent complexes in the Cretaceous offshore rift section of the Campos Basin, offshore Brazil. *Marine and Petroleum Geology,* 74**,** 12-25.

ALVES, T. M., CARTWRIGHT, J. & DAVIES, R. J. 2009. Faulting of salt-withdrawal basins during early halokinesis: Effects on the Paleogene Rio Doce Canyon system (Espirito Santo Basin, Brazil). *Aapg Bulletin,* 93**,** 617-652.

ALVES, T. M., FETTER, M., LIMA, C., CARTWRIGHT, J. A. & STRUGALE, M. 2017. An incomplete correlation between pre-salt topography, top reservoir erosion, and salt deformation in deep-water Santos Basin (SE Brazil). *Marine and Petroleum Geology,* 79**,** 300-320.

ANDRESEN, K. J. 2012. Fluid flow features in hydrocarbon plumbing systems: What do they tell us about the basin evolution? *Marine Geology,* 332**,** 89-108.

BARKER, P. 1983. Tectonic Evolution and Subsidence History of the Rio Grande Rise. *Initial reports of the deep sea drilling project 72***,** 953 - 976.

BARRY, C., MCBRIDE, PAUL, WEIMER, MARK, G. & ROWAN 1998. The effect of allochthonous salt on the petroleum systems of northern Green Canyon and Ewing Bank (offshore Louisiana), northern Gulf of Mexico. *AAPG Bulletin,* 82**,** 1083-1112.

BERTONI, C. & CARTWRIGHT, J. 2015. Messinian evaporites and fluid flow. *Marine and Petroleum Geology***,** 165-176.

BERTONI, C. & CARTWRIGHT, J. A. 2007. Major erosion at the end of the Messinian Salinity Crisis: evidence from the Levant Basin, Eastern Mediterranean. Basin Research, 19, 1-18.

BERTONI, C., KIRKHAM, C., CARTWRIGHT, J., HODGSON, N. & RODRIGUEZ, K. 2017. Seismic indicators of focused fluid flow and crossevaporitic seepage in the Eastern Mediterranean. *Marine and Petroleum Geology,* 88**,** 472-488.

BORCHERT, H. & MUIR, R. O. 1964. Salt deposits: the origin, metamorphism and deformation of evaporites. Van Nostrand, 1964.

CARTWRIGHT, J. 2011. Diagenetically induced shear failure of fine-grained sediments and the development of polygonal fault systems. Marine and Petroleum Geology, 28, 1593-1610.

CARTWRIGHT, J., JAMES, D. & BOLTON, A. 2003. The genesis of polygonal fault systems: a review. Geological Society, London, Special Publications, 216, 223-243.

CARTWRIGHT, J., HUUSE, M. & APLIN, A. 2007. Seal bypass systems. *AAPG bulletin,* 91**,** 1141-1166.

CARTWRIGHT, J., KIRKHAM, C., BERTONI, C., HODGSON, N. & RODRIGUEZ, K. 2018. Direct calibration of salt sheet kinematics during gravity-driven deformation. Geology, 46, 623-626.

CARTWRIGHT, J., KIRKHAM, C., FOSCHI, M., HODGSON, N., RODRIGUEZ, K. & JAMES, D. 2021. Quantitative reconstruction of pore-pressure history in sedimentary basins using fluid escape pipes. Geology, 49, 576-580.

CARTWRIGHT, J. A. & LONERGAN, L. 1996. Volumetric contraction during the compaction of mudrocks: a mechanism for the development of regional-scale polygonal fault systems. Basin Research, 8, 183-193.

CHANG, H. K., KOWSMANN, R. O., FIGUEIREDO, A. M. F. & BENDER, A. 1992. Tectonics and stratigraphy of the East Brazil Rift system: an overview. *Tectonophysics,* 213**,** 97-138.

DANDO, P. R., AUSTEN, M. C., BURKE, R. A., KENDALL, M. A., KENNICUTT, M. C., JUDD, A. G., MOORE, D. C., O'HARA, S. C. M., SCHMALIJOHANN, R. & SOUTHWARD, A. J. 1991. Ecology of a North Sea pockmark with an active methane seep. *Marine Ecology Progress Series,* 70**,** 49-63.

DAVISON, I. 2009. Faulting and fluid flow through salt. *Journal of the Geological Society,* 166**,** 205-216.

DOOLEY, T. P., JACKSON, M. P. A., JACKSON, C. A. L., HUDEC, M. R. & RODRIGUEZ, C. R. 2015. Enigmatic structures within salt walls of the Santos Basin—Part 2: Mechanical explanation from physical modelling. *Journal of Structural Geology,* 75**,** 163-187.

FENG, Y. E., STEINBERG, J. & RESHEF, M. 2017. Intra-salt deformation: Implications for the evolution of the Messinian evaporites in the Levant Basin, eastern Mediterranean. *Marine and Petroleum Geology***,** 251-267.

FENG, Y. E., YANKELZON, A., STEINBERG, J. & RESHEF, M. 2016. Lithology and characteristics of the Messinian evaporite sequence of the deep Levant Basin, eastern Mediterranean. Marine Geology, 376, 118-131.

FIDUK, J. C., BRUSH, E. R., ANDERSON, L. E., GIBBS, P. B. & ROWAN, M. G. Salt Deformation, Magmatism, and Hydrocarbon Prospectivity in the Espirito Santo Basin, Offshore Brazil. GCSSEPM, 2004.

FIDUK, J. C. & ROWAN, M. G. 2012. Analysis of folding and deformation within layered evaporites in Blocks BM-S-8 and -9, Santos Basin, Brazil. Geological Society, London, Special Publications, 363, 471-487.

Flambard, A. R., Keiling, C., Fusban, H. U., & Marx, G. (1986). Leaching of actinides and fission products from ILW embedded in cement and bitumen, and their mobility in natural salt rock (No. PTB-SE--14).

FRANçA, R. L., DEL REY, A. C., TAGLIARI, C. V., BRANDãO, J. R. & FONTANELLI, P. D. R. 2007. Bacia do Espírito Santo. *Boletim de Geociencias da PETROBRAS,* 15, 501-509.

GAMBOA, D., ALVES, T., CARTWRIGHT, J. & TERRINHA, P. 2010. MTD distribution on a 'passive' continental margin: The Espirito Santo Basin (SE Brazil) during the Palaeogene. *Marine and Petroleum Geology,* 27, 1311-1324.

GAMBOA, D. & ALVES, T. M. 2015. Spatial and dimensional relationships of submarine slope architectural elements: A seismic-scale analysis from the Espírito Santo Basin (SE Brazil). *Marine and Petroleum Geology,* 64, 43-57.

GHANBARZADEH, S., HESSE, M. A., PRODANOVIĆ, M. & GARDNER, J. E. 2015. Deformation-assisted fluid percolation in rock salt. *Science,* 350, 1069-72.

GRISHINA, S., PIRONON, J., MAZUROV, M., SERGEY, G., PUSTILNIKOV, A., FON-DER-FLAAS, G. & GUERCI, A. 1998. Organic inclusions in salt. Part 3. Oil and gas inclusions in Cambrian evaporite deposit from East Siberia. A contribution to the understanding of nitrogen generation in evaporites. *Organic Geochemistry,* 28, 297-310.

HO, S., HOVLAND, M., BLOUET, J. P., WETZEL, A., IMBERT, P. & CARRUTHERS, D. 2018. Formation of linear planform chimneys controlled by preferential hydrocarbon leakage and anisotropic stresses in faulted fine-grained sediments, offshore Angola. Solid Earth, 9, 1437-1468.

HOVLAND, M., RUESLåTTEN, H. & JOHNSEN, H. K. 2015. Red Sea salt formations—a result of hydrothermal processes. The Red Sea. Springer.

HOVLAND, M., RUESLåTTEN, H. & JOHNSEN, H. K. 2018a. Large salt accumulations as a consequence of hydrothermal processes associated with 'Wilson cycles': A review Part 1: Towards a new understanding. Marine and Petroleum Geology, 92, 987-1009.

HOVLAND, M., RUESLåTTEN, H. & JOHNSEN, H. K. 2018b. Large salt accumulations as a consequence of hydrothermal processes associated with 'Wilson cycles': A review, Part 2: Application of a new salt-forming model on selected cases. Marine and Petroleum Geology, 92, 128-148.

HOVLAND, M., RUESLåTTEN, H. & JOHNSEN, H. K. 2019. Salt Formation, Accumulation, and Expulsion Processes During Ocean Rifting—New Insight Gained from the Red Sea. Geological Setting, Palaeoenvironment and Archaeology of the Red Sea. Springer.

HOVLAND, M., RUESLåTTEN, H. G., JOHNSEN, H. K., KVAMME, B. & KUZNETSOVA, T. 2006. Salt formation associated with sub-surface boiling and supercritical water. Marine and Petroleum Geology, 23, 855-869.

HOVLAND, M., GARDNER, J. V. & JUDD, A. G. 2010. The significance of pockmarks to understanding fluid flow processes and geohazards. *Geofluids,* 2**,** 127-136.

HOVLAND, M. & JUDD, A. 1988. *Seabed pockmarks and seepages: impact on geology, biology, and the marine environment*, Springer.

HOVLAND, M., RUESL?TTEN, H. G., JOHNSEN, H. K., KVAMME, B. & KUZNETSOVA, T. 2006. Salt formation associated with sub-surface boiling and supercritical water. *Marine and Petroleum Geology,* 23, 855-869.

HüBSCHER, C., CARTWRIGHT, J., CYPIONKA, H., LANGE, G. J. D. & URAI, J. L. 2007. Global Look at Salt Giants. *Eos Transactions American Geophysical Union,* 88.

HUDEC, M. R. & JACKSON, M. P. A. 2007. Terra infirma: Understanding salt tectonics. *Earth-Science Reviews,* 82, 1-28.

HUUSE, M., JACKSON, C. A. L., VAN RENSBERGEN, P., DAVIES, R. J., FLEMINGS, P. B. & DIXON, R. J. 2010. Subsurface sediment remobilization and fluid flow in sedimentary basins: an overview. *Basin Research,* 22, 342-360.

JACKSON, A. L., JACKSON, M. P. A., HUDEC, M. R. & RODRIGUEZ, C. R. 2014. Internal structure, kinematics, and growth of a salt wall: Insights from 3-D seismic data. *Geology,* 42, 307-310.

JACKSON, C. A. L., JACKSON, M. P. A., HUDEC, M. R. & RODRIGUEZ, C. R. 2015. Enigmatic structures within salt walls of the Santos Basin—Part 1: Geometry and kinematics from 3D seismic reflection and well data. *Journal of Structural Geology,* 75, 135-162.

Jamieson, J.W., Petersen, S. & Bach, W. 2016. Hydrothermalism. In: Harff, J., Meschede, M., Petersen, S., Thiede, J. (eds) Encyclopedia of Marine Geosciences. Encyclopedia of Earth Sciences Series. Springer, Dordrecht.

KERN, P. H. 2001. Development of damage and permeability in deforming rock salt. *Engineering Geology*.

KIRKHAM, C., CARTWRIGHT, J., BERTONI, C. & VAN RENSBERGEN, P. 2020. The genesis of a giant mud canopy by catastrophic failure of a thick evaporite sealing layer. *Geology,* 48**,** 787-791.

KIRKHAM, C., CARTWRIGHT, J., HERMANRUD, C. & JEBSEN, C. 2017. The genesis of mud volcano conduits through thick evaporite sequences. *Basin Research*, 30(2), 217-236.

KIRKHAM, C., CARTWRIGHT, J., JAMES, D. & KEARNEY, L. 2022. Episodic venting of extreme subsalt overpressure through a thick evaporitic seal. Marine and Petroleum Geology, 142.

KOYI, H. A. 2001. Modeling the influence of sinking anhydrite blocks on salt diapirs targeted for hazardous waste disposal. *Geology,* 29**,** 387-390.

LEWIS, S. & HOLNESS, M. 1996. Equilibrium halite-H2O dihedral angles: High rock-salt permeability in the shallow crust? *Geology,* 24**,** 431-434.

LI, J. & MITRA, S. 2020. Seismic models of detachment and faulted detachment folds. *Marine and Petroleum Geology,* 117**,** 104385.

LøSETH, H., GADING, M. & WENSAAS, L. 2009. Hydrocarbon leakage interpreted on seismic data. *Marine and Petroleum Geology,* 26**,** 1304-1319.

MAGEE, C., PICHEL, L. M., MADDEN-NADEAU, A. L., JACKSON, C. A. L. & MOHRIAK, W. 2021. Salt–magma interactions influence intrusion distribution and salt tectonics in the Santos Basin, offshore Brazil. Basin Research, 33, 1820-1843.

OPPO, D., EVANS, S., IACOPINI, D., KABIR, S. M., MASELLI, V. & JACKSON, C. A. L. 2020. Leaky salt: pipe trails record the history of cross-evaporite fluid escape in the northern Levant Basin, Eastern Mediterranean.

PONTES, R. L. B., MAUL, A. R. & SILVA, C. G. 2022. Seismic Characterization of Internal Salt Cycles: A Case Study in the Santos Basin, Brazil. 2022, 39, 15.

POPP, T., KERN, H. & SCHULZE, O. 2001. Evolution of dilatancy and permeability in rock salt during hydrostatic compaction and triaxial deformation. *Journal of Geophysical Research*: Solid Earth, 106(B3): 4061-4078.

ROWAN, M. G., URAI, J. L., FIDUK, J. C. & KUKLA, P. A. 2019. Deformation of intrasalt competent layers in different modes of salt tectonics. *Solid Earth,* 10**,** 987-1013.

SCHLEDER, Z., URAI, J. L., NOLLET, S. & HILGERS, C. 2008. Solution-precipitation creep and fluid flow in halite: a case study of Zechstein (Z1) rocksalt from Neuhof salt mine (Germany). *International Journal of Earth Sciences,* 97**,** 1045-1056.

SCHOENHERR, J., URAI, J. L., KUKLA, P. A., LITTKE, R., SCHLéDER, Z., LARROQUE, J. M., NEWALL, M. J., AL-ABRY, N., AL-SIYABI, H. A. & RAWAHI, Z. 2007. Limits to the sealing capacity of rock salt: A case study of the infra-Cambrian Ara Salt from the South Oman salt basin. *AAPG Bulletin,* 91**,** 1541-1557.

SMODEJ, J., REUNING, L., BECKER, S. & KUKLA, P. A. 2019. Micro- and nano-pores in intrasalt, microbialite-dominated carbonate reservoirs, Ara Group, South-Oman salt basin. *Marine and Petroleum Geology,* 104**,** 389-403.

STOLT, R. H. & BENSON, A. K. 1986. Seismic Migration: Theory and Practice. *Pergamon*.

STROZYK, F., GENT, H. W. V., URAI, J. L. & KUKLA, P. A. 2012. 3D seismic study of complex intra-salt deformation: An example from the Upper Permian

Zechstein 3 stringer, western Dutch Offshore. *Geological Society London Special Publications,* 363**,** 489-501.

SZATMARI, P., MORé DE LIMA, C., FONTANETA, G., DE MELO LIMA, N., ZAMBONATO, E., MENEZES, M. R., BAHNIUK, J., COELHO, S. L., FIGUEIREDO, M., FLORENCIO, C. P. & GONTIJO, R. 2021. Petrography, geochemistry and origin of South Atlantic evaporites: The Brazilian side. Marine and Petroleum Geology, 127, 104805.

TEDESCHI, L. R., JENKYNS, H. C., ROBINSON, S. A., SANJINéS, A. E. S., VIVIERS, M. C., QUINTAES, C. M. S. P. & VAZQUEZ, J. C. 2017. New age constraints on Aptian evaporites and carbonates from the South Atlantic: Implications for Oceanic Anoxic Event 1a. *Geology***,** 45(6): 543-546.

TEIXEIRA, L., LUPINACCI, W. M. & MAUL, A. 2020. Quantitative seismic-stratigraphic interpretation of the evaporite sequence in the Santos Basin. Marine and Petroleum Geology, 122.

Van Gent H, Urai J L, De Keijzer M. The internal geometry of salt structures–a first look using 3D seismic data from the Zechstein of the Netherlands. Journal of Structural Geology, 2011, 33(3): 292-311.

WARREN & KEITH, J. 2016. Salt usually seals, but sometimes leaks: Implications for mine and cavern stabilities in the short and long term. *Earth-Science Reviews,* 165**,** 302-341.

ZE, T. & ALVES, T. M. 2016. The role of gravitational collapse in controlling the evolution of crestal fault systems (Espírito Santo Basin, SE Brazil). *Journal of Structural Geology,* 92**,** 79-98.

ZE, T. & ALVES, T. M. 2021. Localized strata-bound domino faulting offshore Espírito Santo Basin (southeastern Brazil): The case for sudden release of fluid in salt-withdrawal basins. AAPG Bulletin, 105, 1535-1562.

Figure and table captions

Figure 1. Location of the study area and observed fluid-flow features. a) The red box shows the 3D seismic volume used in this study, which is located in the compressional domain of Espírito Santo Basin at a water depth ranging from 1500 m to 2000 m. b) Variance map of the study area (-3284 ms twt) showing main salt structures, i.e. salt ridges stretching in a SW-NE direction and salt diapirs. Yellow stars are the locations of where gas chimneys and active salt intrusions are observed. Location of seismic sections in the research are marked with the dashed lines.

Figure 2. Seismic stratigraphy of the study area. Horizon 5 represents a high-amplitude positive seismic reflection on the modern seafloor. Horizon 1 represents the crest of the salt structure. The upper Unit 4 is a mud-rich succession. Unit 3 represents an interval of volcaniclastic material deposited from the Eocene to Late Oligocene. Horizons 2, 3 and 4 are main regional unconformities formed during the Paleocene to Late Oligocene. Location of the seismic section is shown in Figure 1. P-wave velocity data for ODP Site 516 was taken from Barker et al. (1983).

Figure 3. Uninterpreted (a-d) and interpreted seismic sections (e-h) showing fluid flow features in supra-salt successions formed on top of main salt structures and intra-salt seismic reflections. Supra-salt fluid flow anomalies comprise gas chimneys (e-h), bright spots (some of which are interpreted as free gas accumulations) (e-h), dissolution pockmarks on top of salt structures (e and g), and anomalies associated

with polygonal faults (a). Intra-salt anomalies comprise dissolution-related (pushed-down) seismic reflections (a) continuous strata reflecting impure salt, and continuous intra-salt sediment packages of high amplitude (e-h). e) A system of pushed-down, high-amplitude reflections within the salt overhang, upright gas chimney, polygonal fault system and bright spots on top of the gas chimney. f-g) Upright gas chimney, and bright spots on top of the gas chimney. h) Upright gas chimney and bright spots, which are located on top and beside the gas chimney.

Figure 4. Interpreted seismic section showing key geological features in the study area, including intra-salt high-amplitude anomalies, pushed-down reflections, pockmarks on the crest of salt structures, gas chimneys, polygonal faults, and bright spots.

Figure 5. Fluid flow features and associated elements associated with the fluid-flow system shown in Fig. 3e. a) A polygonal system developed in supra-salt strata. b) Dissolution pockmarks on the crest of the interpreted salt structure, with diameters of ~ 1200 m and ~ 500 m, respectively. c-d) Thickness map of Unit 1 (H1 -H2) and Unit 2 (H2 - H3) show drastic thinning of areas on top of the dissolution pockmarks, the area is sufficiently larger than the size of the dissolution pockmarks.

Figure 6 Seismic section showing layered, and deformed intra-salt structures, and bright spots in supra-salt successions.

Figure 7. Uninterpreted and interpreted seismic sections show a fluid flow system with a buried salt intrusion. Seismic section show clear truncation that salt intrude into the supra-salt strata. On top of the salt intrusion, bright spots is observed. Apart from the bright spot observed on top of the salt intrusion, this phenomenon is also observed in the strata at the same burial depth of ‘free gas’ as determined for the study area.

Figure 8. Uninterpreted and interpreted seismic sections showing active salt intrusion associated with crestal fault in the study area. Active salt intrusion is revealed to follow a main crestal fault developed in the study area (defined as a border fault by Ze and Alves, 2016), shaping the modern seafloor. A tilted gas chimney is also observed, proving the multi-phased salt activities affecting in the study area. The dashed yellow line indicates the relative location of the border fault. The active salt intrusion has a smaller overburden thickness than the gas chimneys observed in Figs. 3 and 5.

Figure 9. Seismic section (a) and root-mean-square (RMS) amplitude maps (b-d) showing intra-salt high-amplitude anomalies. High-amplitude and continuous reflections within salt are clearly highlighted on RMS amplitude maps, marking the presence of clastic sediments or anhydrite layers. Either of these lithologies can potentially generate large volumes of fluid, significantly changing the physical properties of salt giants.

Figure 10. Seismic section (a) and root-mean-square (RMS) amplitude maps (b-c) showing intra-salt high-amplitude anomalies. High-amplitude reflections within salt are clearly presented and interpreted by RMS amplitude maps, which reflect lithologically-heterogeneous salt structures.

Figure 11. Conceptual models for salt seal failure. a) Active subsalt fluid percolation into a salt structure through connected pore networks in the lower part of the salt structures. b) Oil and gas generated from the maturation of organic matter within the salt, and/or water generated from hydrite dewatering process comprise. c) Fluid transferred into the salt structures through slabs that extend from the salt withdrawal basins. With a significant volume of fluid within salt structures, dissolution-related fluid flow into supra-salt strata is the main mechanism for salt-seal failure.

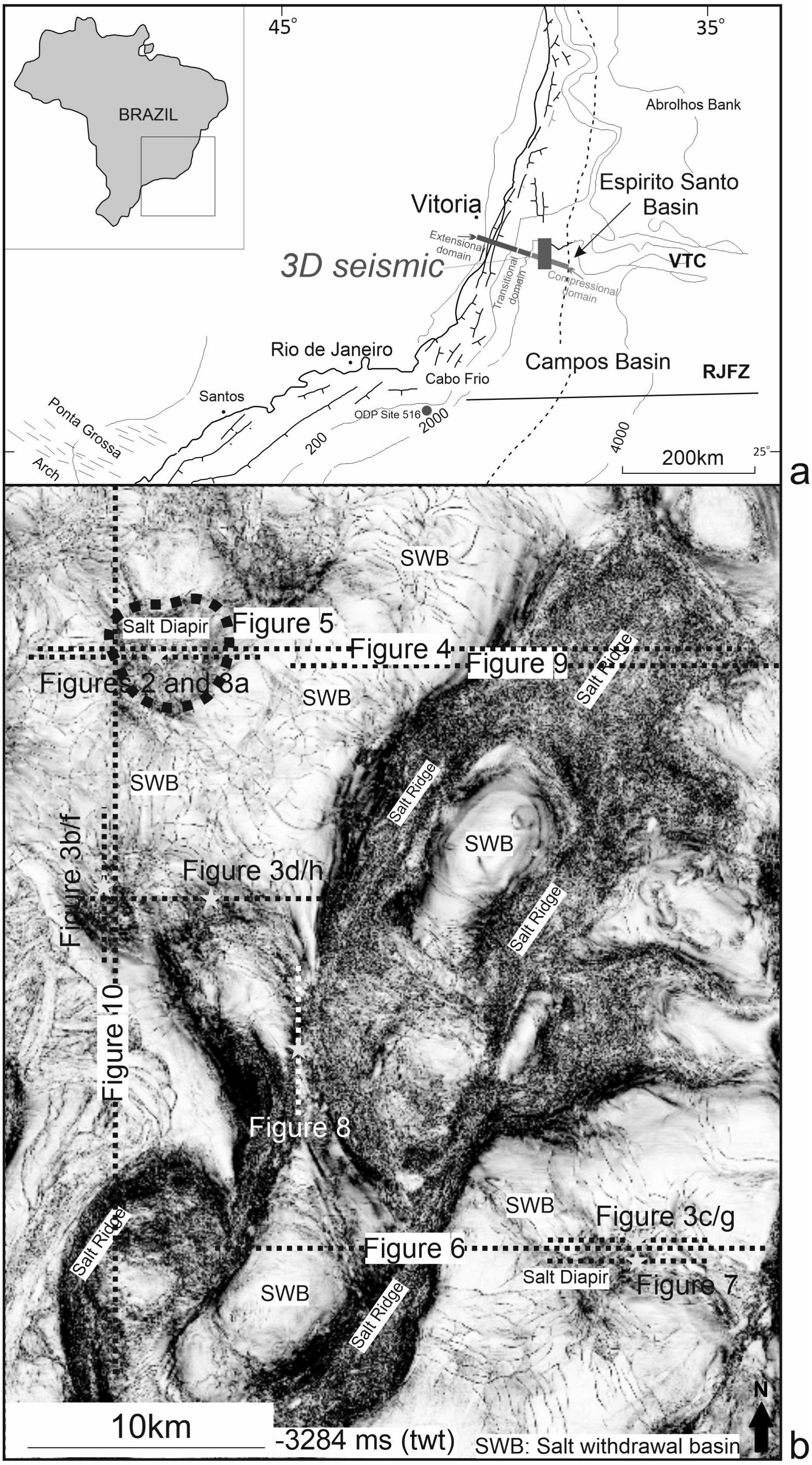
BRAZIL
45°
35°
Abrolhos Bank
Espirito Santo Basin
Vitoria
Extensional domain
Transitional domain
Compressional domain
3D seismic
VTC
Rio de Janeiro
Cabo Frio
Campos Basin
RJFZ
Santos
Ponta Grossa Arch
ODP Site 516
2000
200
4000
25°
200km
a
SWB
Salt Diapir
Figure 5
Figure 4
Figure 9
Figures 2 and 8a
Salt Ridge
Figure 3b/f
Figure 3d/h
Figure 10
Figure 8
Figure 3c/g
Figure 6
Figure 7
10km
-3284 ms (twt)
SWB: Salt withdrawal basin
N
b

Fig. 1

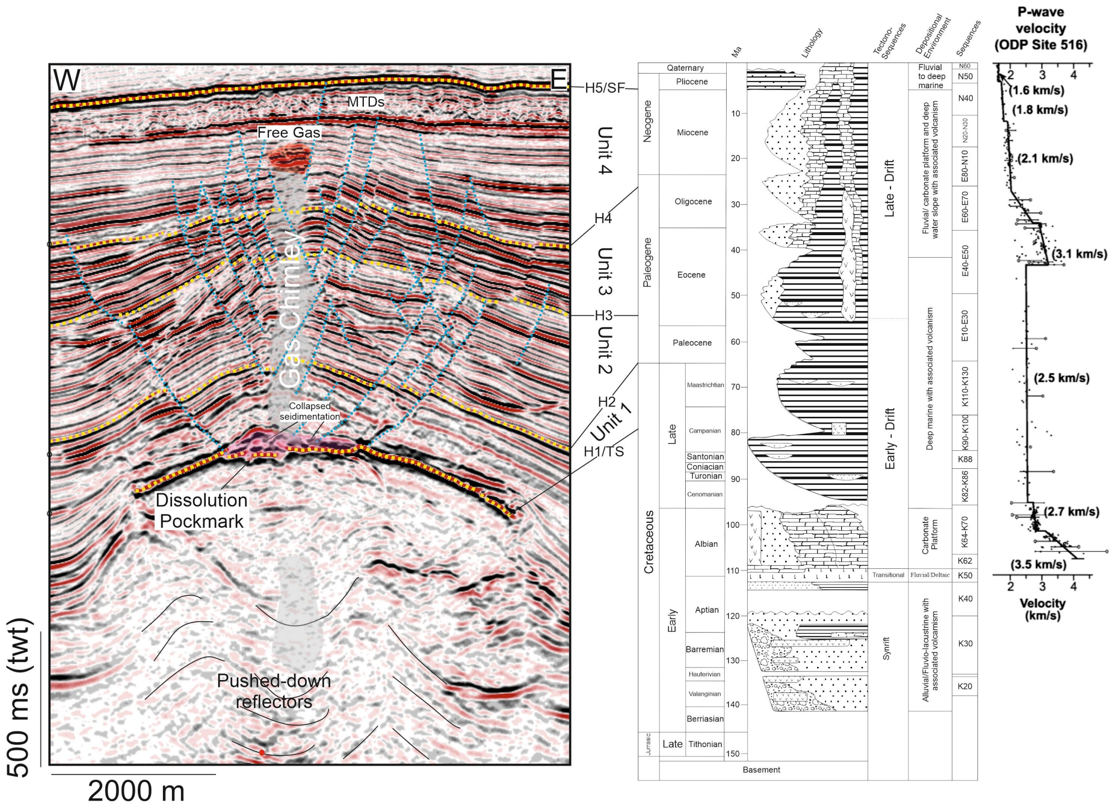

W
E
H5/SF
MTDs
Free Gas
Gas Chimney
Unit 4
H4
Unit 3
H3
Unit 2
H2
Unit 1
H1/TS
Collapsed seidimentation
Dissolution Pockmark
Pushed-down reflectors
500 ms (twt)
2000 m
Ma
Lithology
Tectono-Sequences
Depositional Environment
Sequences
Neogene
Paleogene
Cretaceous
Late - Drift
Early - Drift
Synrift
Basement
P-wave velocity (ODP Site 516)
Velocity (km/s)

Fig. 2

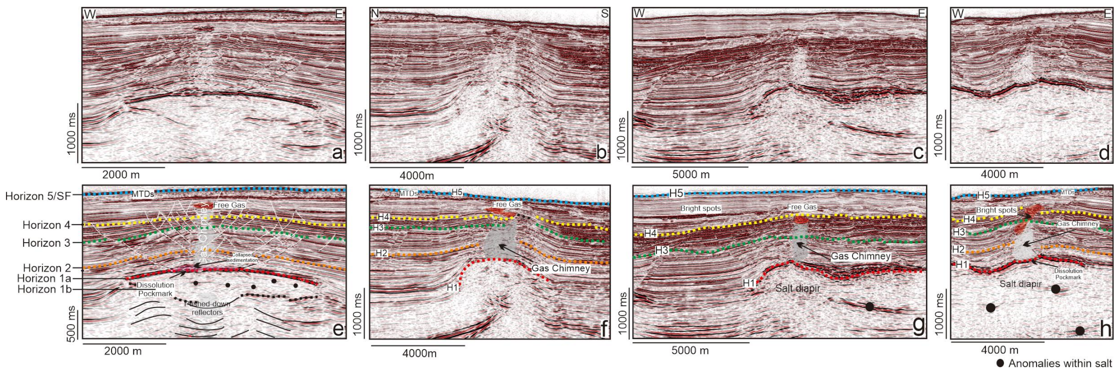

Horizon 5/SF
Horizon 4
Horizon 3
Horizon 2
Horizon 1a
Horizon 1b
Free Gas
Gas Chimney
Salt diapir
Bright spots
Anomalies within salt

Fig. 3

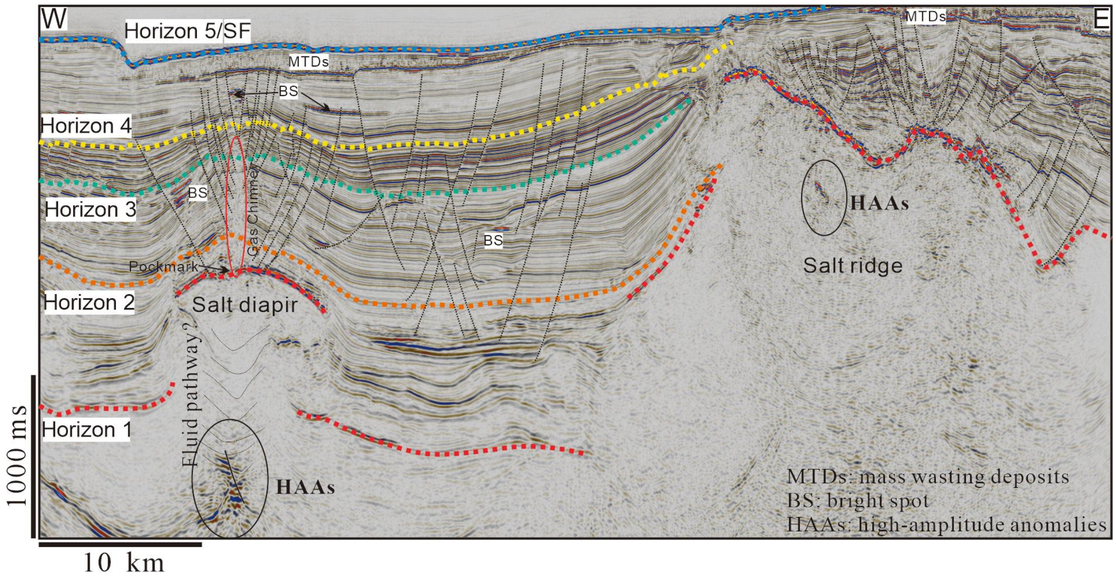
W
E
Horizon 5/SF
MTDs
BS
Horizon 4
Horizon 3
BS
Gas Chimney
BS
Pockmark
Horizon 2
Salt diapir
Fluid pathway?
Horizon 1
HAAs
HAAs
Salt ridge
1000 ms
10 km
MTDs: mass wasting deposits
BS: bright spot
HAAs: high-amplitude anomalies

Fig. 4

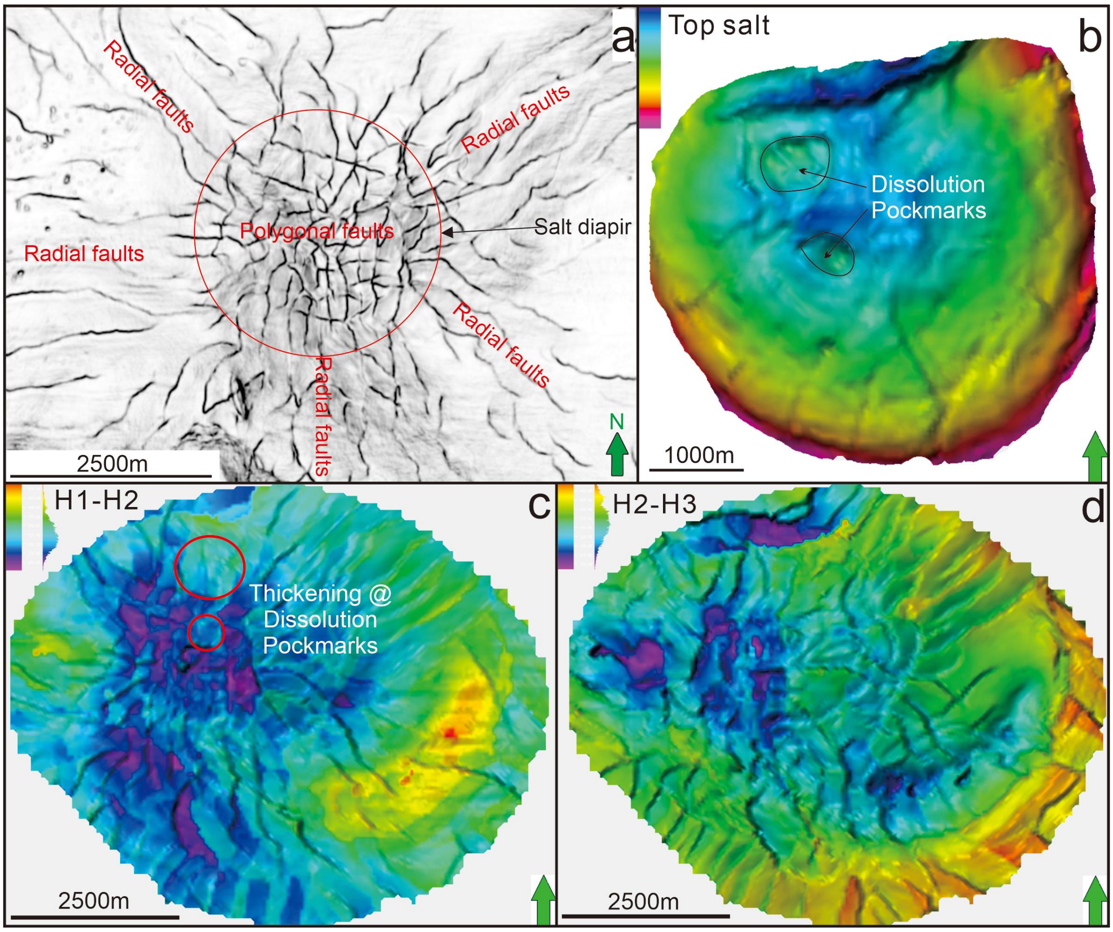
a
Radial faults
Radial faults
Radial faults
Polygonal faults
Salt diapir
Radial faults
Radial faults
N
2500m
Top salt
b
Dissolution
Pockmarks
1000m
H1-H2
c
Thickening @
Dissolution
Pockmarks
2500m
H2-H3
d
2500m

Fig. 5

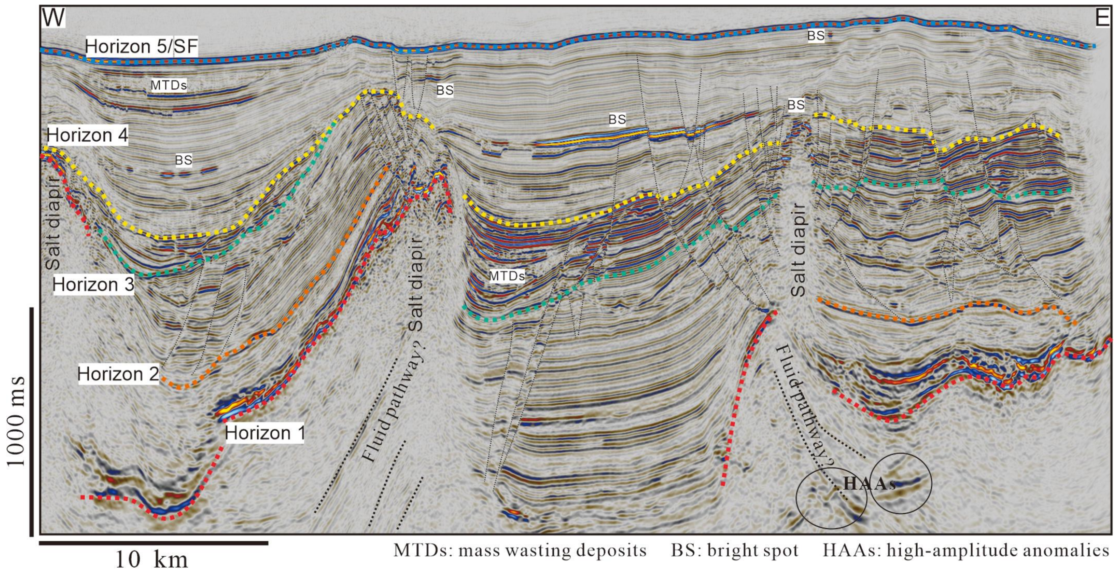

W
E
Horizon 5/SF
MTDs
BS
Horizon 4
Salt diapir
Horizon 3
Horizon 2
Horizon 1
Fluid pathway?
Salt diapir
MTDs
HAAs
1000 ms
10 km
MTDs: mass wasting deposits BS: bright spot HAAs: high-amplitude anomalies

Fig. 6

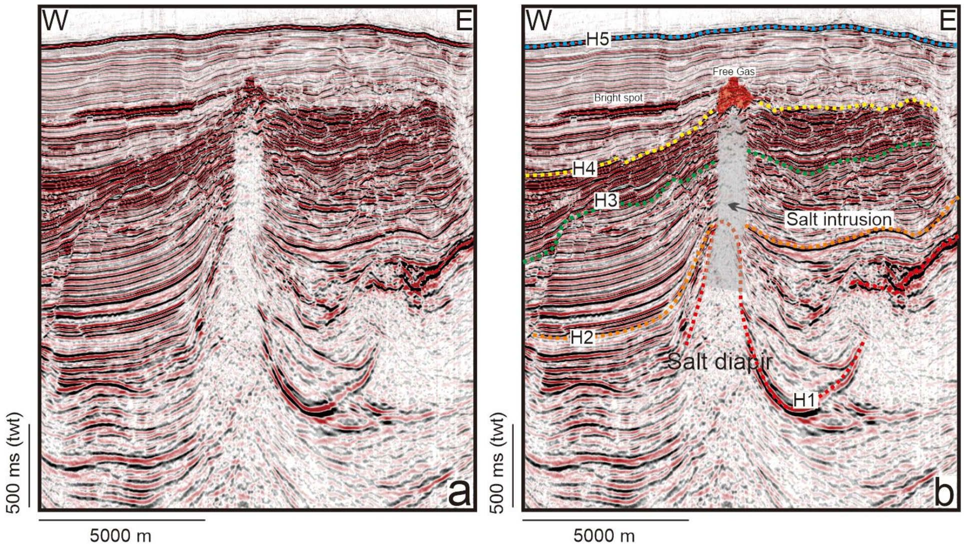

W
E
a
b
H5
Free Gas
Bright spot
H4
H3
Salt intrusion
H2
Salt diapir
H1
500 ms (twt)
5000 m

Fig. 7

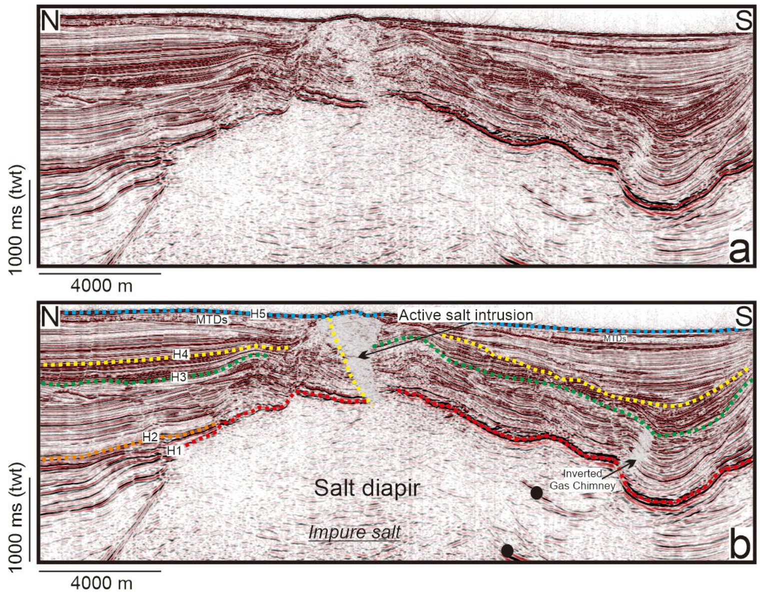
N
S
1000 ms (twt)
4000 m
a
H5
MTDs
Active salt intrusion
H4
H3
H2
H1
MTDs
Salt diapir
Impure salt
Inverted Gas Chimney
b

Fig. 8

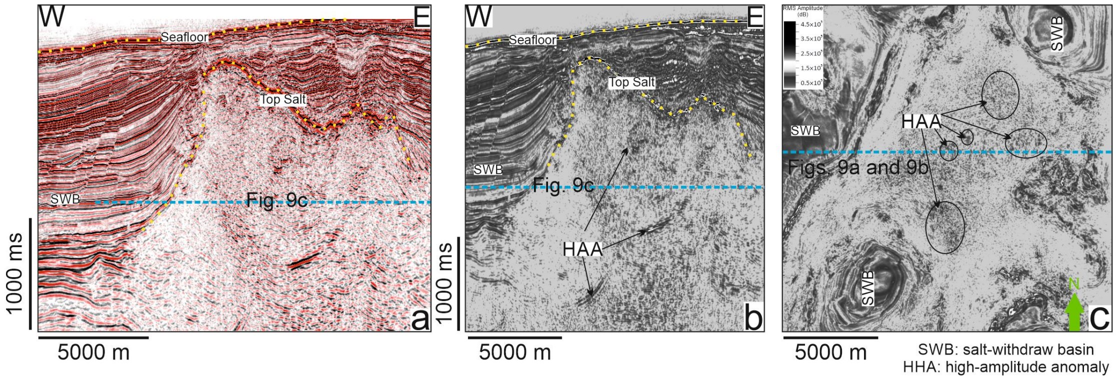
W
E
Seafloor
Top Salt
SWB
Fig. 9c
1000 ms
5000 m
a
HAA
b
Figs. 9a and 9b
c
SWB: salt-withdraw basin
HHA: high-amplitude anomaly

Fig. 9

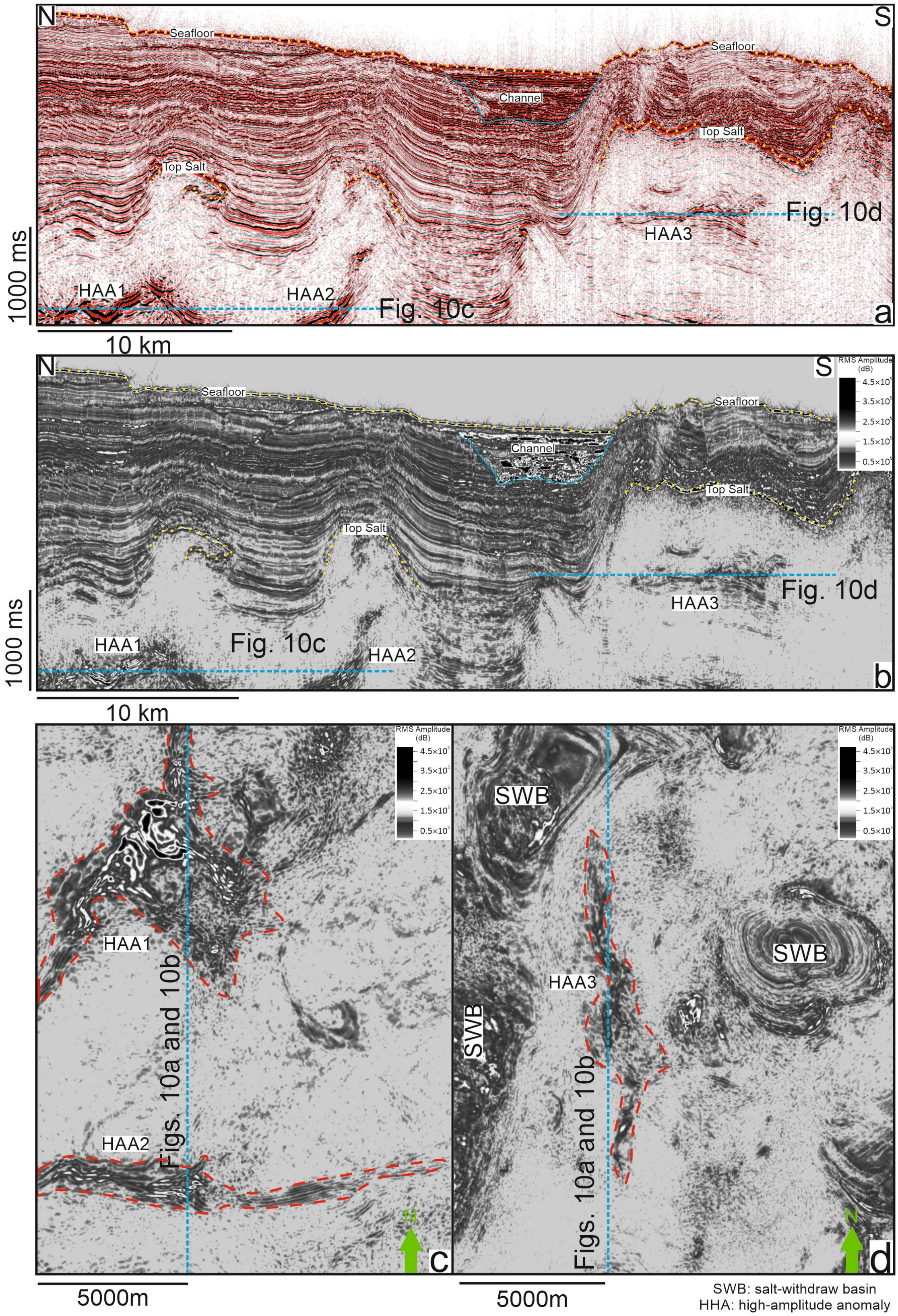

832

833 Fig. 10

834

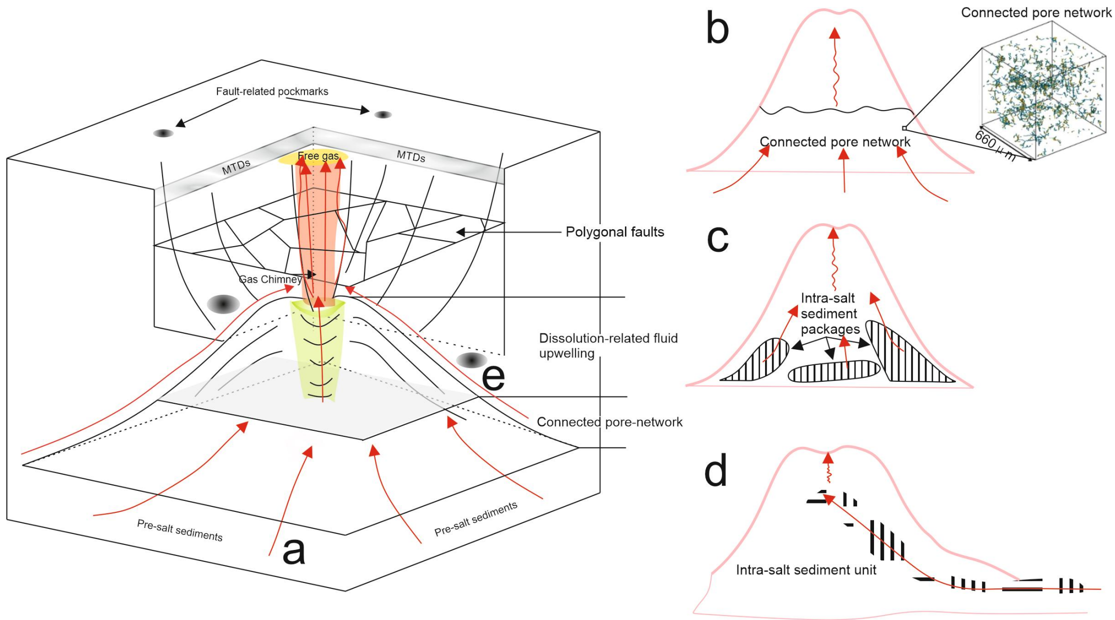

835 Fig. 11